JOURNAL OF MATERIALS SCIENCE 33 (1998) 4349–4356

Biaxial monotonic and fatigue fracture of some commercial ABS and PVC sheets

A. G. ATKINS, G. JERONIMIDIS, S. ARNDT
Department of Engineering, University of Reading, Reading RG6 6AY, UK
Email: A.G.Atkins@reading.ac.uk

Biaxial loading of pre-cracked cruciform testpieces has been preformed in a novel rig attached to a uniaxial testing machine. Fracture toughness R or δ_c of the ductile acrylonitride butadiene styrene (ABS) and polyvinyl chloride (PVC) determined by the Cotterell–Mai method is dependent on remote biaxiality. Least toughness is shown for equibiaxial tension; greatest for uniaxial tension. These monotonic fracture results may be modelled using void growth mechanics. Fatigue crack growth rates also depend on remote biaxiality. Paris/Walker representation of the data shows that the slopes n of $\log(da/dN)$ versus $\log \Delta K$ do not change much, but the constant of proportionality C decreases as the tensile mean stress increases. There may be a connection between the biaxial-dependent C and R or δ_c.

1. Introduction

While plastic flow under combined stresses has been studied for many polymers (pressure-dependent anisotropic yield criteria, etc. (e.g. [1] for a review)), there is very little information available for biaxial fracture and low and high cycle fatigue of polymers. Standard texts on polymers [e.g. 2, 3] have essentially no information of this sort. In the literature, Leevers and co-workers [4, 5] looked at high cycle fatigue of polymethylmethacrylate (PMMA) and polyvinylchloride (PVC), where da/dN for PMMA reduced somewhat at tensile biaxialities but where there was no apparent effect for PVC; Takemori [6] investigated fatigue of discs impacted by a plunger, data from which was analysed in traditional S-N terms. This lack of data is rather surprising given the known effects of biaxiality on fracture and fatigue of metals [7–9] and given the possibility of molecular orientation at crack tips in polymers where local properties are not only different from bulk properties but are locally anisotropic as well; the propagation of cracks, their energetic stability and directional stability must all depend on this sort of thing. Given the lack of information, one is led to wonder what criteria are used in the design of polymer pipelines, shell structures, pressure vessels, containers, storage vessels and such like which operate under biaxial loading. It would appear that it is often assumed that the "second stress" has no effect on fracture and fatigue. Yet the presence of an applied transverse stress can markedly change the shape of the in-plane shear stress contours in the near vicinity of the crack tip [10]. This must affect molecular orientation patterns at crack tips and crack initiation and propagation.

The paucity of biaxial data can hardly be a result of disinterest. Rather it may be caused by perceived practical difficulties of testing. Conventional biaxial testing machines, using four independently controlled actuators (or two with linkages) to keep the test section of cruciform specimens stationary, are expensive. Sometimes uniaxially loaded specimens, having inclined cracks, are employed to get mixed tensile and shear (modes I and II) cracks but such specimens cannot provide simple biaxial stresses in varying ratios. Again tubular specimens (stressed in various combinations of internal/external pressure, axial and torsional loads) have been used, with and without starter cracks, and a range of biaxialities are possible. However, material has to be available in tubular form and there can be end-pressure-sealing problems. Reviews of different specimens for biaxial testing, with advantages and disadvantages and the ranges of biaxialities attainable (sometimes very limited in practice), are given in [8, 9].

There is a simple and inexpensive way of achieving *biaxial* loading on a standard uniaxial tensile testing machine, which we now use routinely at Reading. The idea was proposed for testing aircraft fabrics in the First World War and was described in *Flight* Magazine in 1919 [11]. Fig. 1 shows how different tensile biaxialities are achieved by orientating the cruciform at different angles in the testing machine. For example, a 45° set-up produces a 1 : 1 tensile loading; 30° a 1.73 (perpendicular to the ligament) : 1 (parallel to the ligament); 60° a 0.59 : 1 loading. Table I gives the loading ratios for different angles with respect to the axis of the tensile testing machine. Fears that superimposed bending would detract from the simplicity of the method have been allayed by experiments and finite element calculations [12], and indeed bending seems hardly significant until quite large displacements are imposed as shown by tests on gridded neoprene sheet rubber

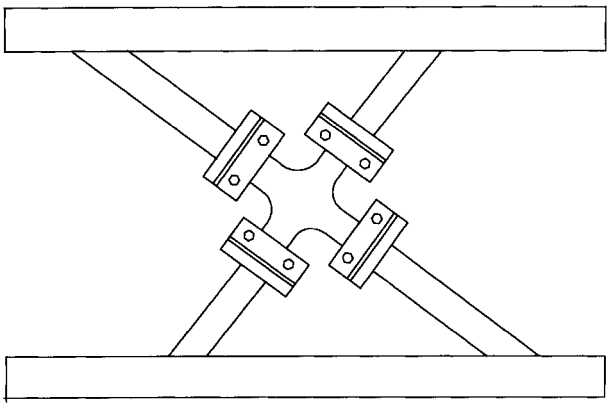

Figure 1 Different orientations of test rig with respect to pulling axis of uniaxial testing machine to give different biaxiality ratios.

TABLE I Load ratios at different angles with respect to testing machine axis.

Orientation, θ	Load ratio, λ
0°	uniaxial (∞)
30°	1.73 : 1
35°	1.43 : 1
40°	1.19 : 1
45°	1 : 1
50°	0.84 : 1
55°	0.70 : 1
60°	0.58 : 1

samples; uniform biaxial loading is produced in the centre of the testpiece.

Different-length loading rods have to be used with each loading ratio, for which there are appropriate attachment holes in the loading frame. Of course, orientations of $(45^\circ + \theta)$ and $(45^\circ - \theta)$ use the same pairs of rods, but swapped orthogonally. Each pair of rods is strain-gauged and calibrated for load; checks were made to confirm that the total load given by the the uniaxial testing machine corresponded with the resolved components from along the loading rods

$$P_{\text{total}} = P_{\perp\text{crack}} \cos\theta + P_{||\text{crack}} \sin\theta \quad (1)$$

The biaxiality ratio is given by the force resolution perpendicular to the axis of the testing machine

$$P_{||\text{crack}} \cos\theta = P_{\perp\text{crack}} \sin\theta \quad (2)$$

$$P_{\perp\text{crack}}/P_{||\text{crack}} = \cot\theta \quad (3)$$

Greater and smaller ratios than those given in Table I, while possible, involve very long connecting rods and the whole device becomes extremely wide. Note that the rig permits situations where the loading parallel to the crack can be greater than the loading perpendicular to the crack.

In the work described in this paper we used cruciform testpieces having two cracks along the centre lines of the "transverse arms" to leave a ligament in the centre of the specimen directly across the line of action of the "axial" load (Fig. 2). In this way we have the equivalent of the "deep double edge notch" (DENT) specimen loaded across the ligament, but now additionally side-loaded parallel to the ligament. It is possible to have a centre-cracked cruciform testpiece, but experiments show that the ends of the cracks do not always propagate along the ligament, except for the severest biaxiality ratios.

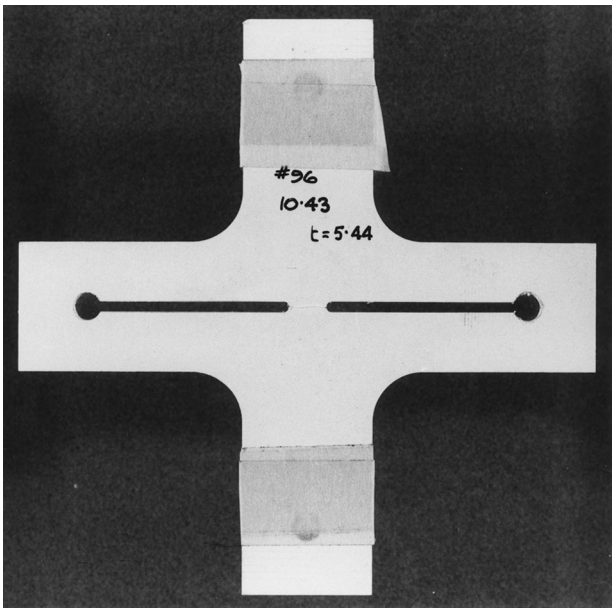

Figure 2 Typical cruciform double-edge notch testpiece.

The choice of DENT cruciform testpieces is also influenced by the Cotterell–Mai method of analysis for monotonic ductile fracture toughness which is employed in this investigation, which was originally established for DENT testpieces loaded uniaxially [13–15]. The essential features of the test method are: (i) to measure the work done U in breaking different length ligaments (the distance L between the ends of the starter cracks); (ii) to plot that work normalized by Lt (where t is the thickness of the sheet) versus L; and (iii) to determine the fracture toughness from the ordinate intercept of the plot. A complementary analysis is to determine the critical crack opening-displacement (COD, δ_c) by back extrapolation of a plot of the load-point-displacement at final fracture (δ_f) versus L. The theory behind this second method of analysis may be found in Cotterell and Mai [16].

Commercial acrylonitrile butadiene styrene (ABS) and PVC samples were used for both monotonic and fatigue measurements. The ABS sheets were 1.5 mm and 5 mm thick; the PVC was 3 mm thick. The 1.5-mm ABS had a yield strength of some 25 MPa and UTS of 36 MPa; for the 6 mm ABS, the corresponding results were some 24 MPa and 32 MPa. Both thicknesses were essentially isotropic (see Table II). The PVC samples drew down in the tensile test, with peak stress before necking of some 46 MPa and drawing stress of 35 MPa. The sheets were again isotropic for all practical purposes.

2. Experimental results

2.1. Monotonic loading

When the ligament breaks under the biaxial loading, the load drops. However, unlike the uniaxial DENT

TABLE II Tensile tests on 6-mm thick ABS

Specimen no.	1	2	3	4	5	6	7	8	9
Orientation (degrees)	0	0	0	45	45	45	90	90	90
Width (mm)	30.15	30.04	30.03	30.09	30.10	30.11	30.06	30.11	30.04
Yield load (kN)	4.60	4.48	4.39	4.28	4.23	4.35	4.40	4.45	4.51
Yield stress (MPa)	25.43	24.87	24.38	23.72	23.39	24.05	24.38	24.63	25.02
Strain at yield (%)	4.17	4.00	3.83	3.83	4.05	4.00	3.89	3.75	3.83
Maximum load (kN)	5.92	5.90	5.90	5.66	5.62	5.50	5.80	5.92	5.95
UTS (MPa)	32.74	32.71	32.76	31.36	31.11	30.43	32.18	32.75	33.01
Strain at UTS (%)	6.41	6.31	6.34	5.98	6.34	5.92	6.26	6.11	6.13
Energy to failure (J)	44.72	33.65	29.70	52.96	43.00	27.32	89.32	70.64	41.38
Failure strain (%)	10.90	8.74	7.78	12.96	10.97	7.66	19.92	15.65	9.92

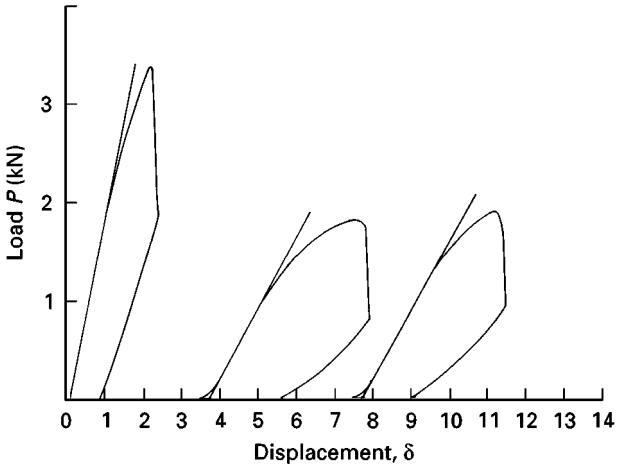

Figure 3 Typical P–δ plots from cruciform testpieces, in this case 3 mm PVC ($\lambda = 0.58:1$).

test where the two halves of the specimen can separate and where in consequence the load drops to zero, the load drops only a certain amount when using cruciform testpieces owing to the restraining effect, after ligament fracture, of the two side arms which remain unbroken at the grips. To obtain the work dissipated in fracture, the testpieces are unloaded on the testing machine, to give load–displacement (P–δ) diagrams, such as shown in Fig. 3.

There are, of course, three P–δ diagrams to inspect, namely: (i) the testing machine total load versus crosshead displacement (corrected for machine stiffness); and the pair of P–δ diagrams for the loads (ii) across the uncracked ligament; and (iii) parallel to the uncracked ligament. An interesting question arises as to *what* work area should be used for U in biaxial Cotterell–Mai U/Lt versus L plots, namely: is it the total work done as given by the testing machine autograph trace; or is it merely the work done perpendicular to the crack; or is it even some combination of the components of work done perpendicular and parallel to the crack? When the investigation commenced, we were not sure and, as will be evident from the results given later, different answers are given by these different possible interpretations of U. The question was resolved with the use of displacement gauges along and perpendicular to the uncracked ligament. It showed that the load-point displacement parallel to the crack essentially ceases at crack propagation (or at necking if that precedes cracking in ductile materials) and that no external work is done in the transverse direction during propagation. Thus the dissipated work U for use in the Cotterell–Mai U/Lt versus L plots, from which the biaxial R are obtained, is that done *perpendicular* to the uncracked ligament. The work done, in the zone of plasticity around the ligament, by loads parallel to the uncracked ligament before fracture, causes microstructural damage in the region where the crack eventually propagates. The magnitude of this effect depends upon the biaxiality, and hence the fracture toughness R will change with biaxiality.

2.2. Fatigue loading

Biaxial DENT testpieces, the same as shown in Fig. 1, were cyclically loaded between zero (in reality a slightly positive load) and fixed fractions of the monotonic failure loads of the testpiece in the same orientations. The cycling rate was some 15 c.p.m. As the setting of the testing machine was load-based and as, in consequence, the deflection increased as the crack length propagated, the cycling rate reduced to some 10 c.p.m. by the end of a typical test. The proportions of the failure load used in fatigue were 50, 32 and 25% for ABS specimens, and 50 and 25% for PVC specimens. In fatigue testing, loads both perpendicular and parallel to the crack fluctuate simultaneously owing to the design of the biaxial rig. It is not possible in this arrangement to fix the load on one axis and cycle the load on the other axis.

The growth of cracks in fatigue was monitored using JVC TKS 350 video cameras with time-lapse recorders. Crack growth occurred from both ends of the uncracked ligament, the cyclically-growing cracks approaching one another until final fracture occurred across the remaining ligament, at the maximum cyclic load. Final fracture usually occurred by plastic collapse in these ductile polymers, the final ligament length being given approximately by xL_0 where x is the percentage of the monotonic failure load used in the fatigue test (25, 32 or 50%, as given above) and L_0 is the starting ligament length. Most of the fatigue crack propagation occurred under elastic conditions even so, as evinced for example by stress whitening in PVC occurring only at the final stages of crack meeting across the remaining ligament. It was unusual for observable cracking to commence simultaneously at

both ends of the ligament. Most often cracking started at one end before the other owing to different notch acuities produced by Stanley blades at the ends of the starter cuts. For purposes of analysis, the two separate crack growths were added and divided by two to give an average crack growth rate (da/dN).

The fatigue data were analysed by determining the crack growth rate (da/dN) and log plotting against ΔK (the range of the applied stress intensity factor), to see if Paris-type relations were followed. Owing to the complicated cruciform geometry and biaxial loading, we used at every biaxiality the simple linear-elastic fracture mechanics (LEFM) Irwin formula for the uniaxially-load DENT testpiece, [17] namely:

$$\Delta K = \Delta\sigma(\pi a)^{1/2}\,[\tan(\pi a/W)/(\pi a/W)]^{1/2} \qquad (4)$$

where $2W$ is the width of a cruciform arm and a the effective length of each edge crack (the starting crack length a_0 being given by $a_0 = W - L_0/2$ where L_0 is the length of the starting ligament); $\Delta\sigma$ is the range of applied stress given by

$$\Delta\sigma = (\sigma_{max} - \sigma_{min}) \approx P_{max}/2WB \qquad (5)$$

with B the thickness of the testpiece.

3. Results

3.1. Monotonic fracture

Fig. 4(a) shows plots of the *total* normalized work versus ligament length for 6.0 mm thick ABS, and Fig. 4(b) shows the work done perpendicular to the fracture versus ligament length from the same data. It is clear that the results "flip-flop" when plotted in these different ways, i.e. normalized total energy (U/Lt) is greatest for lowest biaxiality (highest orientation angle of cruciform testpiece) and least for highest biaxiality (zero angle of orientation), whereas normalized perpendicular energy is greatest for highest biaxiality and least for lowest biaxiality. Furthermore, the slopes of U/Lt versus L plots are different for different biaxialities when total work is employed, becoming steeper for least biaxialities. In contrast the slopes in the perpendicular work plots are almost parallel except for the lowest biaxialities. A similar pattern is observed in the δ_f versus L plots for various thickness materials, where the slopes are parallel, except for the lowest biaxialities, e.g. Fig. 5.

The work perpendicular to the ligament gives, from the ordinate intercepts, the greatest fracture toughness R or δ_c for uniaxial DENT testing with a pattern of decreasing R or δ_c as the sideways loading is increased. Beyond a 1:1 biaxiality (45° orientation of cruciform); however, the toughness changes again. This is caused by crack turning, where at high loads parallel to the ligament, the crack ceases to propagate all the way across the ligament. An extreme example is shown in Fig. 6(a).

Should necking occur across the ligament preceding fracture at low biaxialities, it can happen that "straight-across" fracture occurs for smaller biaxiality than 1:1 (Fig. 6b), but eventually, at even lower biaxialities (greater transverse loads), the cracks will turn and invalidate the results.

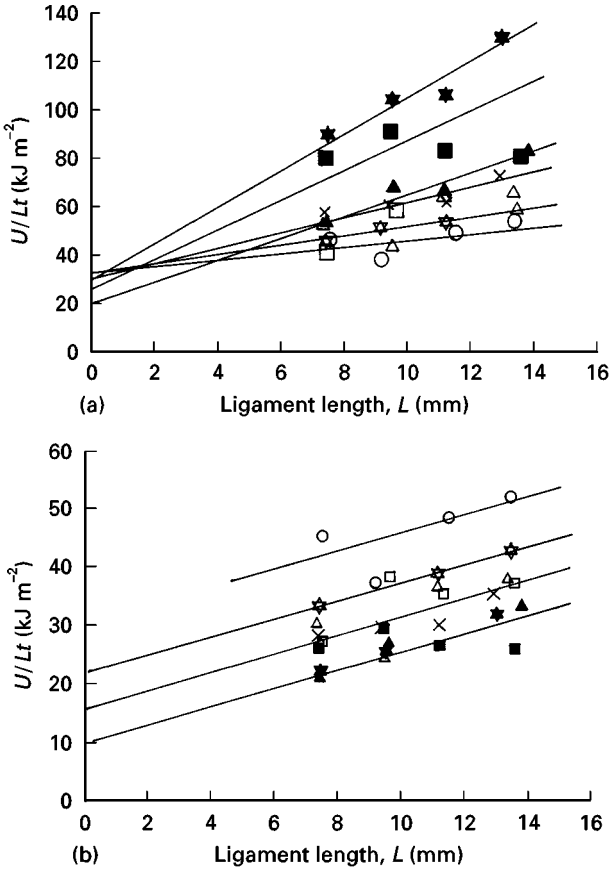

Figure 4 Plots of (a) U_{total}/Lt versus L (✱, 60°; ■, 55°; ▲, 50°; ×, 45°; △, ; □, ; ✡, ; ○) and (b) U_{perp}/Lt versus L (○, 0°; ✡, 30°; □, ; △, ; ×, ; ■, ; ▲, ; ✱,) for for 6-mm thick ABS showing complete reversal of data. Ordinate intercepts give fracture toughness.

Fig. 7 gives the monotonic toughness results for ABS and PVC as a function of load biaxiality.

3.2. Fatigue

Fig. 8(a)–(d) show a set of crack growth data at increasing number of cycles for 1.5 mm thick ABS fatigued at 50% of the monotonic failure load at various biaxialities. Cases where the crack growth at the two ends of the crack ("left" and "right") are almost identical, and where they differ somewhat, are illustrated. Similar patterns were shown for other samples of ABS fatigued at other fractions of the monotonic failure load, and for PVC samples.

Average crack growth rates were obtained from the slopes of the a versus N results, and plotted against the range of applied stress intensity factor, using Equation 1 for ΔK. Fig. 9 gives representative results for ABS and PVC samples, with da/dN in mm/cycle and ΔK in MPa $(m)^{1/2}$. We see that although the slopes n of these Paris plots change little with biaxiality ($n \approx 8$), the constant C in

$$(da/dN) = C(\Delta K)^n \qquad (6)$$

is much affected by biaxiality. In particular, C decreases as the transverse load increases.

Given that different biaxialities produce different mean stresses across the ligament, it was appropriate to investigate the applicability of mean-stress-modified Paris equations. In particular, we looked at

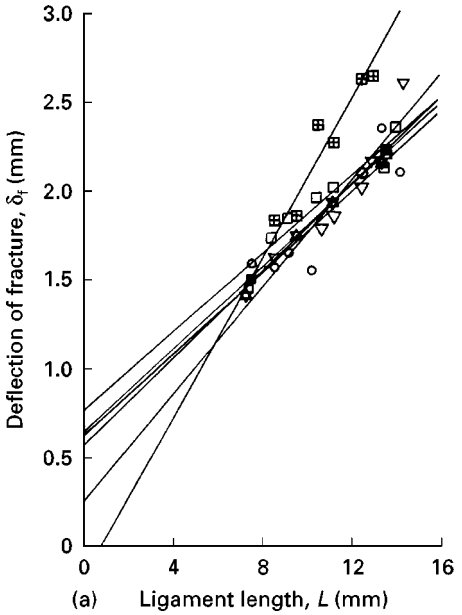

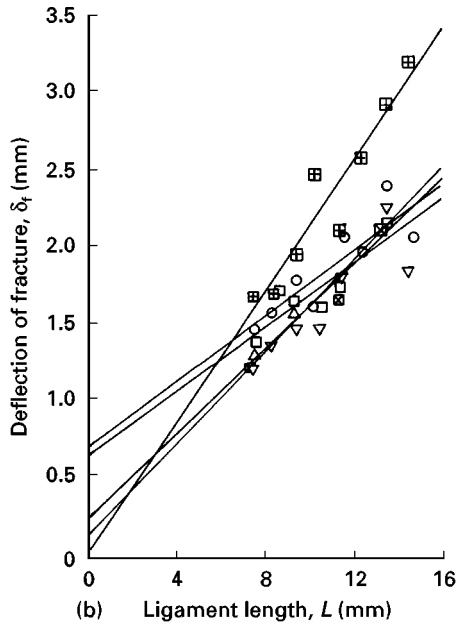

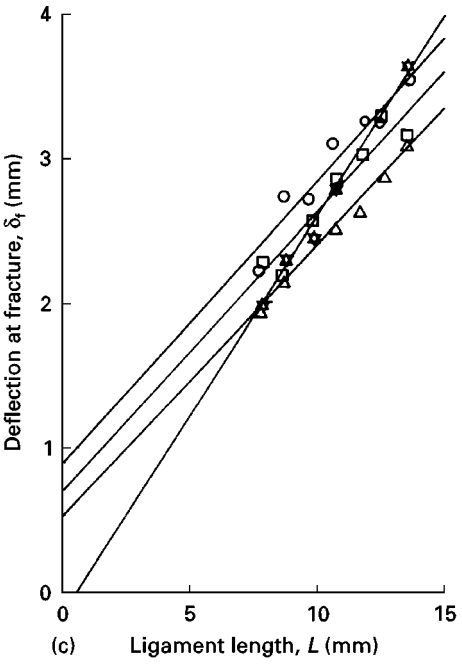

Walker's modification to the Paris relation, [18, 19]

$$\frac{da}{dN} = C'\sigma_{mean}^{m}\Delta K^{n} \tag{7}$$

where $\sigma_{mean} = (\sigma_{max} + \sigma_{min})/2$. In our case, $\sigma_{min} \approx 0$ always, so the equation becomes

$$\frac{da}{dN} = C'(\sigma_{max}/2)^{m}\Delta K^{n} \tag{8}$$

That is, our previous C values become

$$C = C'(\sigma_{max}/2)^{m} \tag{9}$$

Fig. 10 shows log–log plots of C versus $(\sigma_{max}/2)$ for different thicknesses of ABS. The agreement is not too

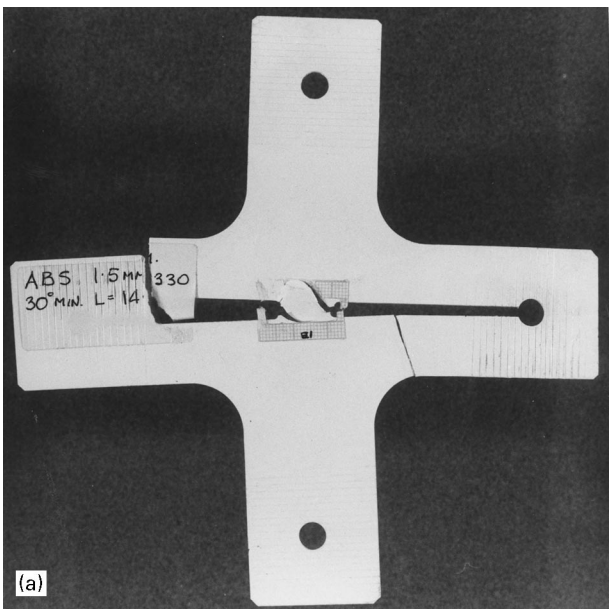

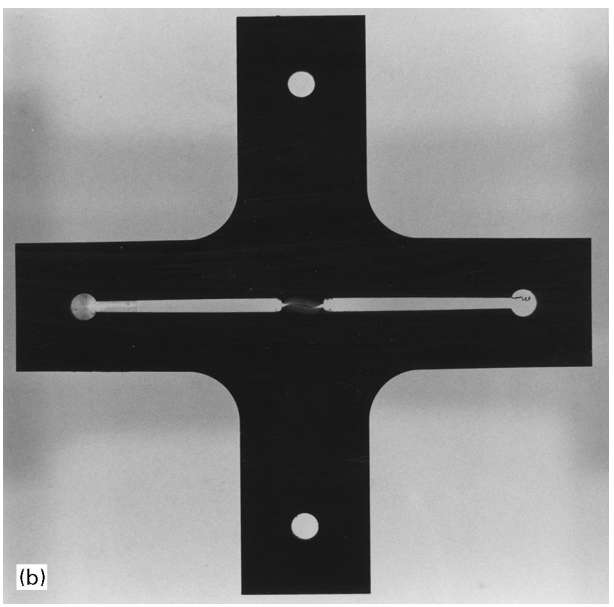

Figure 6 Examples of crack turning under extreme "sideways" loading in 1.5-mm thick ABS.

Figure 5 Plots of δ_f versus L for (a) 6-mm thick ABS; (b) 1.5-mm thick ABS; and (c) 3-mm thick PVC. Ordinate intercepts give COD. ○, 0°; □, 30°; ✡, 40°; ▽, 45°; ◇, 50°; ⊠, 55°; ⊞, 60°.

bad, except for cases where the crack turned where the points do not lie on the line at all. Also, at smallest ($\sigma_{max}/2$), there is some departure from the best fit line. For that line for all ABS data $2\times10^{-2} < C < 10^{-1}$ and $-8 < m < -7$.

We also note that the reduction in C with biaxiality corresponds with the similar reduction in R or δ_c. We have too few data to investigate this properly but, at least for fatigue at small fractions of the monotonic failure load we find

$$C = 2.65\times10^{-4}\,(\delta_c)^{0.8}$$

for 1.5 mm thick ABS fatigued at 25% of the monotonic failure load under various biaxialities (δ_c in mm, C in Equation 5 for da/dN in mm/cycle and ΔK in MPa $(m)^{1/2}$). Also

$$C = 10^{-4}(\delta_c)^{2.4}$$

for 3 mm PVC biaxiality fatigued at 25% of the monotonic failure load.

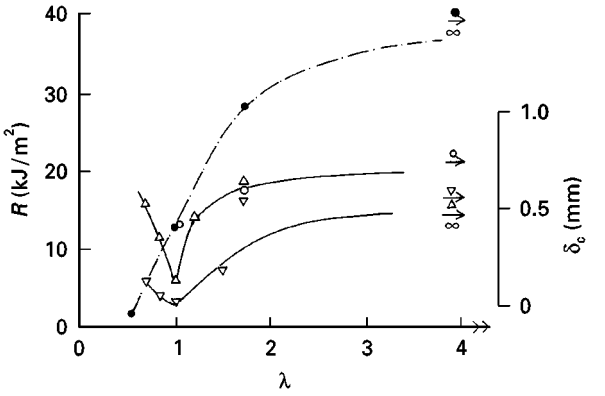

Figure 7 Variation of R and COD with biaxiality. PVC: ●, R; ○, δ_c. ABS: △, δ_c 6 mm, ▽, δ_c 1.5-mm.

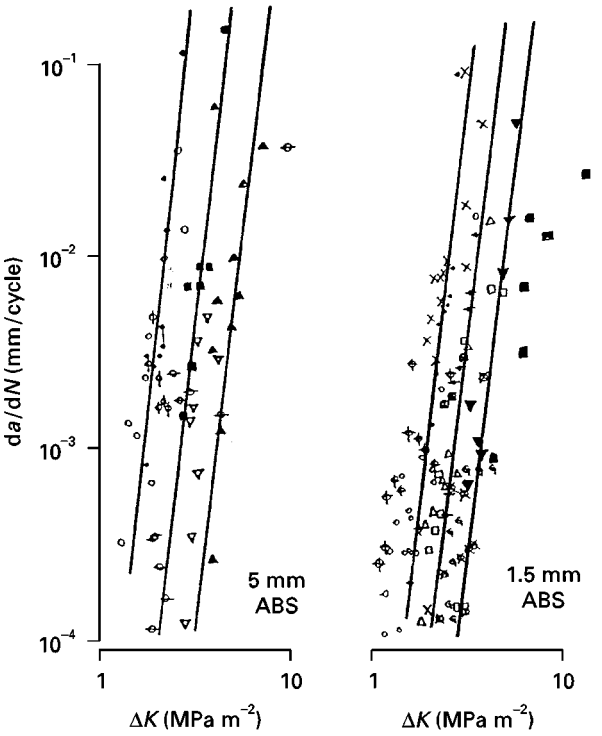

Figure 9 Paris plots of log (da/dN) versus log (ΔK).

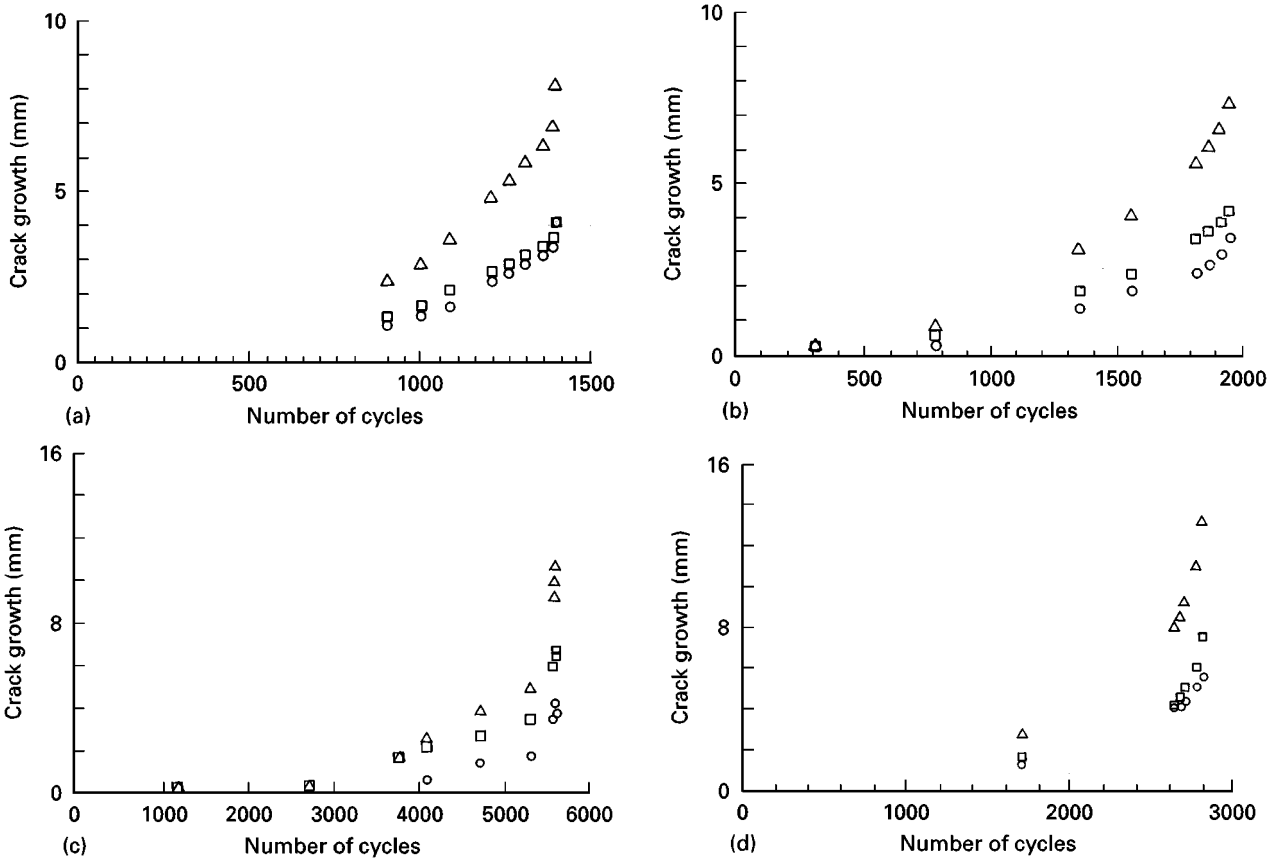

Figure 8 Examples of crack growth in fatigue of 1.5-mm thick ABS, cycled at 50% of monotonic failure load, under different biaxialities. (a) uniaxial (0°, Table I); (b) 1.73 : 1 (30° MAJ); (c) 1 : 1 (45°); (d) 0.58 : 1 (60°, i.e. 30° MIN). ○, left; □, right; △, combined.

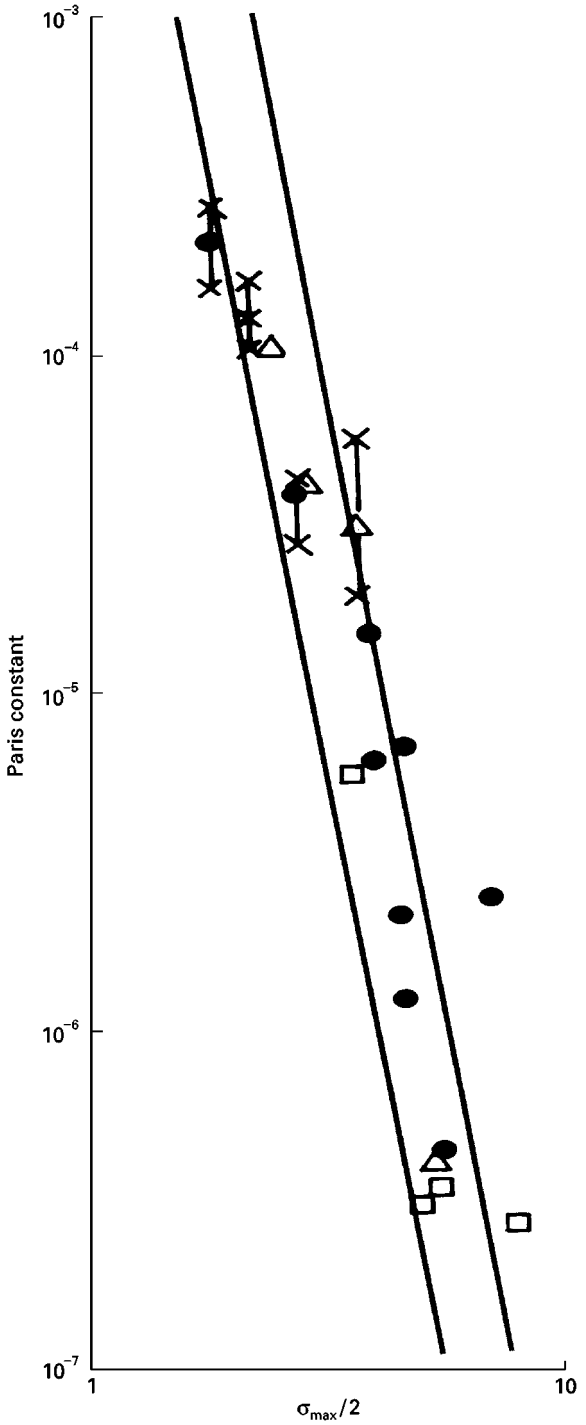

Figure 10 Walker plots of log C_{Paris} versus σ_{mean}.

Insofar as all these relationships come down to micromechanisms and the effect of remote biaxiality on local stresses (particularly hydrostatic stress), the following section is relevant.

4. Model for variation of *R* with biaxiality

Failure in ductile polymers is via micro voiding as can be seen on the fracture surfaces, i.e. lots of fibrils even on macro-brittle surfaces [20]. The distinction between ductile void growth and crazing which is seen in some "brittle" polymers, e.g. polystyrene (PS), PMMA, is often not a clear one. In crazes the zones are in arrays with highly ariated fibrils. We assume that a monotonic fracture occurs by the accumulation of "microstructural damage" to a critical level. Let us assume a generalized damage function given by

$$\int f(\sigma_H/\bar{\sigma})d\bar{\varepsilon} = D \tag{10}$$

where D is accumulated damage, $f(\sigma_H/\bar{\sigma})$ is some function of hydrostatic stress normalized by von Mises stress and $\bar{\varepsilon}$ is von Mises strain. (For polymers whose yielding is pressure-dependent, questions of "normality" of the flow rules associated with the pressure-dependent yield function come in [1] but for present purposes we ignore that; we also presume that the behaviour is isotropic.) At the von Mises strain to fracture $\bar{\varepsilon}_f$ (the upper limit of the integral in Equation 10), the accumulated damage reaches a critical level D_c. The magnitude of D_c is determined from a standard calibration testpiece, such as a simple tension specimen. The lower limit of the integral in Equation 10 is often taken as zero, but there could very well be a cut-off $\bar{\varepsilon}_0$ below which no damage is accumulated; $\bar{\varepsilon}_0$ could be biaxial-dependent too [21], but in the absence of any information on that, we shall take it as constant.

For linear loading paths where the biaxiality ratio $\lambda = \sigma_{\perp crack}/\sigma_{||crack}$, $(\sigma_H/\bar{\sigma})$ is given by [17]

$$(\sigma_H/\bar{\sigma}) = (\lambda + 1)/3(\lambda^2 - \lambda + 1)^{1/2} \tag{11}$$

Thus for uniaxial loading $\lambda = \infty$, and $(\sigma_H/\bar{\sigma}) = 1/3$; for plane strain $\lambda = 2$ and $(\sigma_H/\bar{\sigma}) = (3^{-1/2})$; for equibiaxial tension $\lambda = 1$ and $(\sigma_H/\bar{\sigma}) = 2 \times (3^{-1/2})$. Hence, $f(\sigma_H/\bar{\sigma})$ in the damage function is itself a function of λ, $f(\lambda)$.

In ductile materials undergoing monotonic loading, localized necking often precedes fracture. For example, in the DENT geometry, the ligament may neck down before fracture. Such necks are in plane strain, because the ligament does not shorten during necking. Because $(\sigma_H/\bar{\sigma})$ is always $(3^{-1/2})$ in plane strain, but the $(\sigma_H/\bar{\sigma})$ ratio of the earlier phase of biaxial loading will have been different, (set by the orientation of the cruciform specimen in the testing machine), the damage integral has to be broken down into events before and after necking, i.e. for linear loading paths Equation 10 becomes

$$[f(\sigma_H/\bar{\sigma})(\bar{\varepsilon}_n - \bar{\varepsilon}_0)] + [f(3^{-1/2})(\bar{\varepsilon}_f - \bar{\varepsilon}_n)] = D_c \tag{12}$$

at fracture, with $f(\sigma_H/\bar{\sigma})$ for the pre-necking stage given by Equation 11.

It has been shown [17] that if crack propagation is viewed as continuous reinitiation, then there is a relationship between $\bar{\varepsilon}_f$ and R in plane stress, namely

$$\bar{\varepsilon}_f = [(n + 1)R/B\sigma_0]^{1/(n+1)} \tag{13}$$

for a material following a $\sigma = \sigma_0\bar{\varepsilon}^n$ stress–strain relation, with B the thickness of the sheet. Because the damage equation gives the dependence of $\bar{\varepsilon}_f$ on biaxiality λ, Equations 10 or 12 and Equation 13 together give the variation of R or δ_c with λ.

Fig. 11 shows how the Rice–Tracey model for void growth, where $f(\sigma_H/\bar{\sigma}) = \exp(3\sigma_H/2\bar{\sigma})$, predicts for 1.5 mm thick ABS the variation of the critical crack

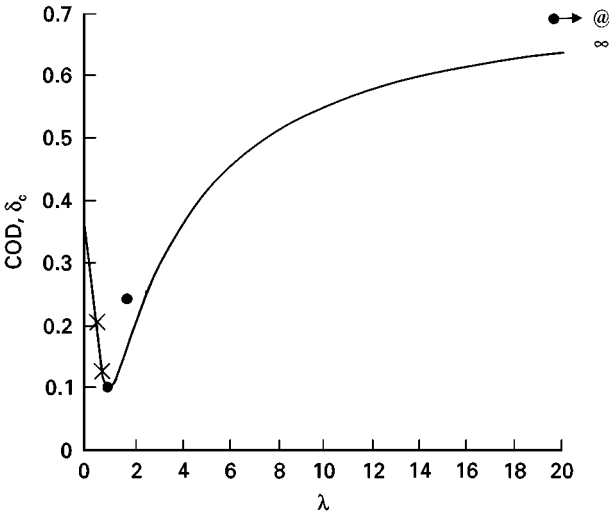

Figure 11 Predictions of Rice–Tracey damage function for variation of monotonic δ_c with remote biaxiality.

opening displacement with remote biaxiality, using Equations 12 and 13 and the relation $R = m\sigma_y\delta_c$. The shape taken by the δ_c versus λ plot is interesting; as the "sideways" loading is increased, i.e. moving from right to left along the abscissa, δ_c decreases and reaches a minimum at $\lambda = 1$. For smaller λ, the curve rises again. (The curve is, in fact, "symmetrical" about $\lambda = 1$ as the biaxiality ratios less than unity correspond with their reciprocals for $\lambda < 1$.) Implicit in this rise in δ_c for $\lambda < 1$ is, however, a presumption that the crack propagates perpendicular to the greater load. For $\lambda < 1$, this means that the crack should turn and the two data points marked "x" did indeed turn during propagation. The agreement is, perhaps, remarkable because the δ_c values are derived from δ_f plots which depend on the ligament breaking right across. This they eventually do for $\lambda < 1$, but only by the two curving cracks finally turning again near the end of propagation to join up and sever the testpiece. In other instances, particularly with metals that neck across the ligament before crack propagation, δ_c values at $\lambda < 1$ are found smaller than the $\lambda = 1$ values, on the downwards extension of the δ_c versus λ ($\lambda > 1$) curve [22]. Even so, at small enough λ, however, the δ_c values rise again. Clearly this requires much more investigation.

5. Conclusions

A novel test rig, permitting biaxial tensile loading in a uniaxial testing machine, has been used for both monotonic and fatigue fracture. In the case of commercial ABS and PVC sheets of various thicknesses, both monotonic ductile fracture toughness and fatigue crack growth rates are affected by the remote biaxial load ratios.

The monotonic toughness is least for equibiaxial tension; it is greatest for uniaxial tension. The toughness behaviour when the load parallel to the DENT testpiece ligament is greater than that perpendicular to it, depends on the extent of the necking along the ligament which precedes cracking: it is possible for even lower toughnesses to be exhibited if the crack does not climb out of the neck "groove". At large enough transverse loads, however the crack turns and climbs out of the "groove" to run approximately perpendicular to the transverse load. That involves greater specific work of fracture. The overall dependency of toughness on remote biaxiality seems to be explicable in terms of void growth mechanics.

Fatigue crack growth rates decrease as the load parallel to the ligament increases. In terms of Paris/Walker type plots, n in $(da/dN) = C(\Delta K)^n$ is more or less unaffected by remote biaxiality, but C decreases with increased transverse loading. The reduction in C corresponds with the reduction in monotonic R or δ_c with remote biaxiality, and there may be a relation but we have too few data to be sure.

Acknowledgements

The work was performed under an EPSRC grant. Thanks are due to K. J. Miller who kindly advised on the approach towards Paris-type plots for biaxial loading. Messrs R. Gladding and J. Frew are thanked for their technical assistance, and C. C. Preston prepared the figures.

References

1. R. RAGHAVA, R. M. CADDELL and A. G. ATKINS, *J. Mater. Sci.* **8** (1973) 1641.
2. J. G. WILLIAMS, "Fracture Mechanics of Polymers" (Ellis Horwood, Chichester 1984).
3. R. W. HERTZBERG and J. A. MANSON, "Fatigue of Engineering Plastics" (Academic Press, New York, 1980).
4. P. S. LEEVERS, J. C. RADON and L. E. CULVER, *Polymer* **17** (1976) 627.
5. P. S. LEEVERS, L. E. CULVER and J. C. RADON, *Engr. Fract. Mech.* **11** (1979) 487.
6. M. T. TAKEMORI, *J. Mater. Sci.* **17** (1982) 164.
7. J. D. EMBURY and G. H. LEROY, *Proc. ICF-4* **1** (1977) 15.
8. H. A. RICHARD, in "Biaxial and Multiaxial Fatigue" (edited by Brown & Miller) EGF Publication 3. MEP, London, 217.
9. E. W. SMITH and K. J. PASCOE, *Fatigue of Engr. Mater & Struct.* **6** (1983) 201.
10. K. J. MILLER and A. P. KFOURI, *Int. J. Fract.* **10** (1974) 393.
11. *Flight*, 1919.
12. A. G. BARBER, Reading University, Dept Engineering, Final Year Project, 1991.
13. B. COTTERELL and J. K. REDDELL, *Int. J. Fract.* **13** (1977) 267.
14. B. COTTERELL and Y. W. MAI, *ibid.* **24** (1984) 229.
15. B. COTTERELL, E. LEE and Y. W. MAI, *ibid.* **20** (1982) 243.
16. B. COTTERELL and Y. W. MAI, "Advances in Fracture Research", ICF-5, Vol. 4, edited by D. Francois. Pergamon, London (1982) p. 1683.
17. A. G. ATKINS and Y. W. MAI, "Elastic & Plastic Fracture" Ellis Horwood, Chichester (1985, 1988).
18. K. WALKER, ASTM STP462, 1, 1970.
19. D. BROEK, "Elementary Engineering Fracture Mechanics" Sijthoff & Nordhoff (1978).
20. J. G. WILLIAMS, Private communication.
21. A. G. ATKINS, In "Fracture Research in Retrospect: Irwin Festschrift" edited by H. P. Rossmanith (Balkema, Rotterdam, 1997) p. 327.
22. A. G. ATKINS and S. ARNDT, to be published.

Received 20 January
and accepted 11 May 1998